Desalination and Water Treatment
www.deswater.com

21 (2010) 238–246
September

1944-3994/1944-3986
doi: 10.5004/dwt.2010.1534

Role of solution hydrodynamics on the deposition of $CaSO_4$ scale on copper substrate

Luai M. Al-Hadhrami, Abdul Quddus*

Research Institute, King Fahd University of Petroleum & Minerals, P.O. BOX 1524, Dhahran-31261, Saudi Arabia
Tel. +96638603533; Fax +96638603996; email: amquddus@kfupm.edu.sa

Received 26 September 2009; accepted 22 May 2010

ABSTRACT

The present investigation highlights the role of solution hydrodynamics on the deposition of calcium sulfate scale on copper substrate. The study was carried out using a Rotating Cylinder Electrode (RCE) system at various pre-set rotational speeds, at 60 and 70°C on 120 and 600 grits polished cylindrical specimens. The effects of temperature, surface roughness, and flow conditions on the deposition of calcium sulfate scale on copper substrate are presented. The results indicate that the solution hydrodynamics play an important role on the rate of deposition of calcium sulfate scale on copper specimens. In addition, the analysis of scaling data further corroborated well with the theoretically predicted diffusion controlled process. Morphology of deposited crystals was obtained from scanning electron microscope (SEM) micrographs and composition was determined with energy dispersive X-ray spectrometer (EDS) method. SEM revealed prismatic needle- and rod-like crystals growth at nucleation sites branching out randomly over the substrate. The secondary growth on the already existing primary crystals of CaSO4 was also seen. EDS confirmed the composition included Ca and S as expected. Furthermore, X-ray diffraction (XRD) analysis of scale showed hemi-hydrate ($CaSO_4 \cdot 1/2H_2O$) form of gypsum.

Keywords: Scale; Calcium Sulfate Scale; $CaSO_4$; Hemihydrate; Gypsum; Copper; $CaSO_4$ on Copper; Rotating Cylinder Electrode; RCE

1. Introduction

The unwanted inorganic minerals and their compounds depositing from process fluid streams on heat transfer surface(s), are called scaling/fouling. These mineral species are sparingly soluble and strongly adhering to the surface of heat transfer equipment that cause major problems to the processing industries worldwide because of related frequent shutdowns and sometimes catastrophic failures. In addition, corrosion products, particulate matters, bio-mass, sludge and slime deposits are other serious problems encountered by these industries. The thermal efficiency of the heat transfer equipment is reduced and process operations disrupted due to these undesired deposits that lead to uncontrollable pressure fluctuations. These altogether create a hazardous situation which may cause fatal accidents, and economic losses. In heat exchangers, scaling of tubes substantially reduces their ability to exchange heat effectively. In desalination plants, the scale deposits affect both the quality and quantity of desalted potable water. In oil producing wells the deposition of alkaline earth sulfates and carbonates scaling compounds restrict flow through tubing strings and hence drastically decrease oil production. Thus, the decrease in thermal efficiency and/or loss of

*Corresponding author

production, results in decline of revenues [1,2]. Moreover vis-à-vis, the concomitant effect of both the scale and corrosion remain challenging problems for plant designers as well as operators [3].

Laboratory methods to study scale deposition generally involve: (a) static experiments, using glassware [2,4–6], and (b) dynamic experiments, involving once through flow rigs or closed re-circulating type flow loops [2,7–11]. Static experiments are relatively easy to perform and, if desired, seeded growth of crystals can also be achieved [5–6]. Static experiments are useful as a first approximation of scaling conditions. Flow loop experiments, on the other hand, simulate industrial situations encountered in actual operations, but are tiresome to perform and require persistent monitoring along with an abundant supply of feedstock solution.

An easy approach to overcome the above mentioned wearing situation (i.e., rigorous monitoring and copious solution) and to conduct laboratory scale formation experiments, is the use of rotating cylinder electrode (RCE) or rotating disk electrode (RDE) systems. The RCE and RDE techniques are well-established methods for studying kinetics of corrosion [12–16] and electrodeposition [17,18]. These techniques have been utilized for the study of scale deposition [19–26] to a limited extent.

We selected RCE for our experimental study for the assessment of the rate of scale deposition, as compared to RDE. RCE has geometrical analogy to pipe surface, and the cylindrical surface of RCE specimen provides more surface area than a round flat disk. These advantages motivated us to opt for the RCE. No attempts were made to study the electrochemical aspects in the present work, therefore, only the scale deposition results obtained on copper substrate, using RCE under fluid flow conditions are presented with various other parameters of interest.

Neville et al. [22–24] studied the electrochemical aspects of surface/solution interactions for $CaCO_3$ scale growth and inhibition on a rotating disk electrode made from SS-316L at different rotational speeds. They utilized a well-known oxygen reduction electrochemical technique to assess the formation of scaling on the RDE surface. They showed that the presence of scaling on the samples actually reduced the electroactive surface area of the specimen and the resulting electrochemical current response. With this technique, they found a good correlation between the surface coverage due to scale and the image analysis performed on the surface of scaled and un-scaled samples. They concluded that with the help of this technique, the mechanism of scale formation, and assessment of inhibitors and their interactions on the solid surface can be studied.

Morizot et al. used the technique developed by Neville [22], to study the inhibition of $CaCO_3$ scale on an SS-316 rotating disc electrode surface. They used polyacrylic acid (PAA) as scale control inhibitor to inhibit both bulk precipitation and scale formation on the metal surface, in varying dosages. They evaluated the performance of PAA-inhibitor by the electrochemical technique and found that the efficacy of the inhibitor may be quite varying in relation to the surface deposition and bulk precipitation in the scaling solution.

Chen et al. utilizing the electrochemical technique suggested by Neville [22], studied the $CaCO_3$ scale formation on a rotating disk electrode surface by using three different supersaturated scaling solutions. They showed that the formation of scale on the specimen and the precipitation in the bulk solution are two different processes which depend on the index of supersaturation. Under potentiostatic control, they monitored the surface coverage of the RDE due to scaling. The rate of oxygen reduction and the resulting electrical current diminished with time during their experiments which allowed ascertaining the presence of scaling on the surface of RDE samples while operating the RDE setup.

Singh and Abbas conducted laboratory analyses and characterization on the actual scale samples obtained from oil production fields of Arabian Gulf region. They found that calcium sulfate, strontium sulfate, barium sulfate, and calcium carbonate are the most commonly occurring scales in production facilities within this region.

Earlier work [19–21], reports deposition of barium sulfate, calcium sulfate and calcium carbonate scales on an SS-316 surface obtained at various rotational speeds by using RCE equipment. This work further reports the results of calcium sulfate scale hydrodynamically deposited on copper specimens. The effect of temperature and surface roughness at various Reynolds numbers for calcium sulfate scale on copper substrate is highlighted. In addition, a comparison of $CaSO_4$ scale deposition on copper and stainless steel-316 from literature is also presented.

Scale deposition is a complex process, involving many factors. These include adequate solution supersaturation, temperature, pressure, hydrodynamic conditions of fluid flow system, etc. Nonetheless, the flow dynamics considerably has an effective role in the scale deposition process among these. Therefore, the basic understanding of scale formation and deposition process is essential for an effective fluid/water treatment and scale mitigation program.

The aim of the present investigation was to understand the deposition of mineral scales on commercial grade metallic materials available in the market. Because, copper is one of the construction metal used in the process industries, therefore, it was selected as a

substrate for calcium sulfate scale deposition. Moreover, the experimental parameters adopted in the study present the process industries operating conditions.

2. Experimental

A schematic of an EG&G Princeton Applied Research Rotating Cylinder Electrode test system is shown in Fig. 1. Cylindrical test specimens (1.27 cm dia. and 1.27 cm long) were machined from commercial grade copper rod and their peripheral surface was exposed to the scaling solution. Further details can be found in [19–20].

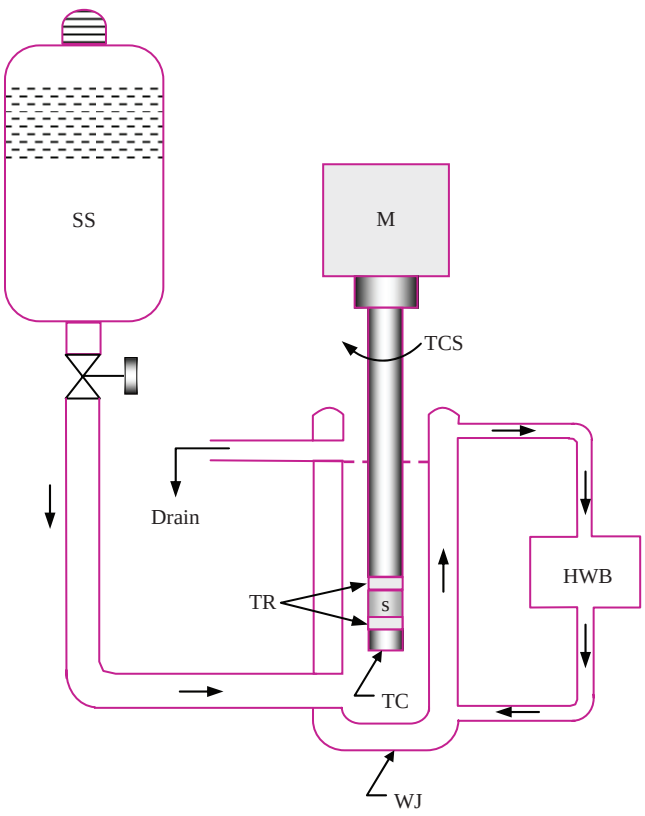

Fig. 1. Schematic of the experimental setup of Rotating Cylinder Electrode equipment.

Analytical grade reagents $CaCl_2$ and Na_2SO_4, were dissolved in deionized water to produce $CaSO_4$ scale by co-precipitation. Concentration of each salt was kept at 0.03 mole/liter. Equal volumes of the two solutions were mixed in a reservoir that was connected to glass test cell, to supply solution at rate of 1 to 1.5 liter/h, so that the composition of scaling solution remains constant. Experiments were conducted on 120 and 600 grit polished cylindrical copper specimens at 60 and 70°C and atmospheric pressure for 6 h duration at various rotational speeds ranging from 100 to 2,000 revolutions per minute (RPM).

The surface texture of the 120 grit and 600 grit polished copper samples was determined by Bendix Linear Profile System (Model 5054). The measurements were performed at 20 $\pm$ 0.5°C and relative humidity (RH) of 40 $\pm$ 5%. The average roughness (Ra) of the test samples was measured both in forward and reverse direction.

The weight gain of scaled samples, after drying in an oven, was measured by an analytical balance with an accuracy of $\pm$ 0.1 mg. The scale deposition rate was calculated by dividing the weight of scale obtained per unit area by the duration of the experiment. A minimum of triplicate experiments were performed at each temperature, surface roughness and rotational speed. Any outlier point if found was repeated to ascertain the result and an average deposition rate for the best of three was taken. The repeatability and uncertainty in the generated data was found to be $\pm$11% as determined by Engineering Equation Solver (EES) software. The induction time was experimentally determined as a function of weight gain verses time for each surface roughness and temperature used in the study.

Morphology of calcium sulfate crystals was studied on flat copper coupons (20 mm $\times$ 8 mm $\times$ 1.5 mm), polished to 120 and 600 grit with silicon carbide (SiC) emery paper. Duplicate specimens were assembled in a Teflon holder that was placed in the test cell and exposed to the calcium sulfate scale forming solution for 1–3 h under the same test conditions. After the tests, the coupons were retrieved, rinsed with distilled water, dried in an oven and preserved for further examination. Scanning electron microscope (JEOL JSM-5800-LV) was used for morphology study and the composition of scale was determined with energy dispersive X-ray spectrometer (EDS) coupled with the microscope. X-ray diffractometer (SHIMADZU-LabX XRD-6000) with CuKα radiation source was used for X-ray diffraction analysis.

3. Results and discussions

3.1. Scale deposition

The measured average surface roughness (Ra value) of 120 grit and 600 grit polished copper samples was

Table 1
Average surface roughness (Ra) values of polished copper specimens

Surface polish (by SiC paper)	Measured average roughness Ra (μ inch)		Maximum average Ra (μ inch)
	Forward Travel	Backward Travel	
600 grit	65	75	75
120 grit	100	115	115

Conversion Factor: 1 μ inch = 0.0254 μm.

115 and 75 micro inch, respectively (Table 1). The lower value of Ra indicates a relatively smooth surface texture having less waviness compared to high value of Ra that refers to large peaks and valleys of the rough surface profile.

The induction period obtained experimentally (weight gain vs. time) for the 120 grit and 600 grit copper polished samples at 60°C was 35 and 45 min, respectively, whilst at 70°C for 600 grit it was 30 min.

Because, scaling/fouling problems are encountered in many industrial processes with normal or incompatible water or with dissolved inorganic salts in water, therefore, some of these salts and their compounds display inverse solubility characteristics. Fig. 2 illustrates the behavior of such normal and inverse solubility salt solutions as proposed by Bott [28]. Two behavioral phenomena of aqueous salt solutions are portrayed in Fig. 2; (a) the cooling of a normal salt solution, and (b) the heating of an inverse solubility salt solution. Case (b) of Fig. 2, i.e., the heating of an inverse solubility salt solution, was adopted in our study and is elaborated as: ''the solution is unsaturated at point A (Fig. 2), as it is heated it reaches the solubility limit at point B (saturation) and then upon further heating to point C, the solution becomes supersaturated. Therefore, at point C, the onset of precipitation occurs from the supersaturated solution, which continues and follows the path up to point D, resulting in increased precipitation, crystallization or scale formation upon continued heating''.

The agitation of supersaturated scaling solution due to the rotation of the specimen at various speeds had a strong impact on precipitation and the rate of mass transport of $CaSO_4$ scale to the electrode surface where it adsorbed and eventually deposited on the surface of the specimens and yielded measurable weight gain of scale on the copper substrate. Analysis of the data was carried out to demonstrate the effect of solution hydrodynamics on the deposition rate of scale. For this, Reynolds numbers were calculated corresponding to each selected rotational speed as suggested by Gabe [16].

The average scale deposition rates obtained at various Reynolds numbers are plotted in Fig. 3 to show the effect of Reynolds numbers on the deposition of calcium sulfate scale on 120 and 600 grit polished copper samples at 60 and 70°C, respectively. The results shown indicate an increase in the rate of deposition verses Reynolds numbers for the data generated in the study and are in agreement with the earlier studies [10–11,19–20].

Fig. 3 further shows the effect of surface finish of copper samples produced with 120 and 600 grit SiC emery papers. The 120 grit polished samples showed comparatively more scale than 600 grit polished samples at 60°C, the increase however, was marginal. An increasing trend in the scaling rate for higher temperature of 70°C is obvious from Fig. 3, as well. In addition, the deposition rate for 600 grit polished sample at the two selected temperatures of 60 and 70°C can also be seen from the figure. At 70°C, the rate of scale deposition increased significantly as compared to 60°C for 600 grit polished copper samples (Fig. 3). A high rate of precipitation is always expected at increased temperature because of inverse solubility characteristics of the supersaturated scale forming solution (Fig. 2). Therefore, more precipitation and deposition of scale was obtained at higher temperature of 70°C on same surface roughness condition, owing to the inverse solubility effect.

We kept the solution's ionic strength (chemistry) constant by replenishing fresh solution to the test cell and varied other parameters of interest, viz.,

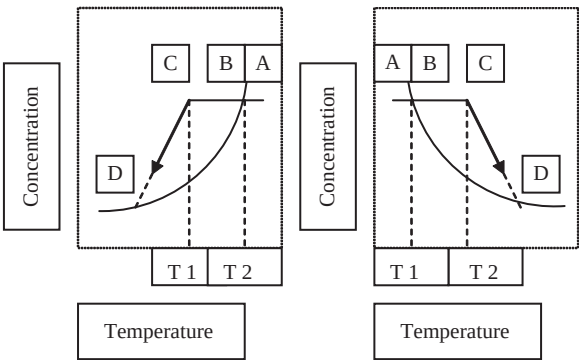

Fig. 2. Behavior of normal and inverse solubility salt solutions [28].

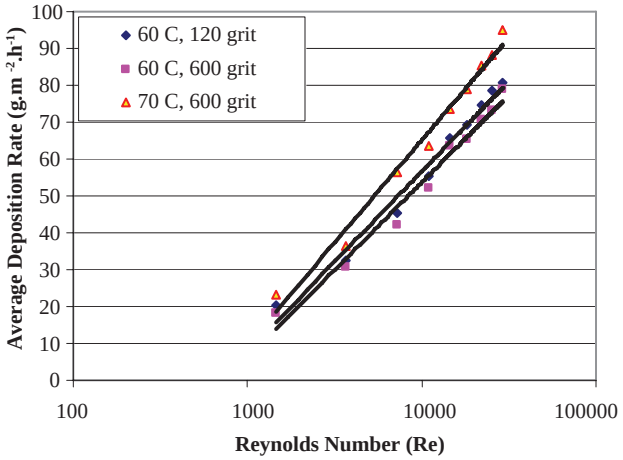

Fig. 3. Average deposition rate of calcium sulfate scale on 120 and 600 grit polished copper as a function of Reynolds Number at 60 and 70°C.

temperature, surface roughness and rotational speed. Albeit, scaling is a complex process, the following explanation, however, provides an overall process of scale deposition in a simple way.

The precipitation of scale from the supersaturated solutions upon heating in the test cell is governed by the double displacement chemical reaction, presented in the equation below:

$$Na_2SO_4\,(aq) + CaCl_2\,(aq) \rightarrow CaSO_4\,(s) + 2NaCl(aq) \quad (1a)$$

The reactants are ionic salts dissolved in water, so the above reaction in ionic form is:

$$Ca^{2+} + SO_4^{2-} + 2H^+ + 2OH^- \rightarrow CaSO_4{\cdot}2H_2O \quad (1b)$$

The resultant product $CaSO_4{\cdot}2H_2O$ (calcium sulfate dihydrate), the mineral called ''gypsum'', is the most commonly found sulfate scale in the oil production environment. The other forms of gypsum are; hemihydrate ''$CaSO_4{\cdot}1/2H_2O$'' and anhydrite ''$CaSO_4$''. All these forms of gypsum potentially cause scaling of oilfield equipment and fouling of heat exchanges. The $CaSO_4{\cdot}2H_2O$ is the most stable form of gypsum that occurs as rock on the earth's crust, however in addition, the hemihydrate and anhydrite gypsum are also naturally found as rock, marble, alabaster, etc., in the earth's crust formations [2]. The combined (bound) water molecule present in the hydrated gypsum can be evaporated upon heating at high temperature leaving behind anhydrous or dehydrated ($CaSO_4$) gypsum [2].

The ionic bond between calcium cations (Ca^{2+}) and sulfate anions (SO_4^{2-}) produces $CaSO_4$ as a precipitated solid phase gypsum (Eq. (1)). Thousands of tiny precipitates called nuclei of $CaSO_4$ conglomerate together (due to surface reaction) in the bulk of scaling solution and after gaining weight deposit on the active nucleation sites present on the surface of the specimen. The nucleation is twofold during scale deposition process. Upon creation of supersaturation., the first nucleation occurs in the bulk of the scaling solution due to chemical reaction (Eq. (1)) whilst, the second nucleation takes place on the surface of the specimen at active nucleation sites present due to surface heterogeneities (kinks, screw-dislocations, scratches, polishing marks, etc.). These surface defects are low energy sites, which attract the precipitating species (diffusion and adsorption) and finally these particles adhere at these active sites on the surface of metal due to mechanical bonding as scale. In addition, the suspended solids, corrosion products, bio-mass, sludge and slime in the flow system can also play an important role in promoting the scale deposition process. A simplified schematic representation of the scale deposition mechanism resulting from cooling water system or process fluid stream is shown in Fig. 4 [2].

In our study the chemical reaction continuously produced precipitation in the bulk solution due to the replenishment of the fresh solution (i.e., constant ionic potential). However, at high rotational speeds, shear forces increase at the solid-liquid interface, so the scale erosion (removal) process may become significant along with the scale deposition process. Secondly at high rotation, the contact time of scale to the surface of specimens becomes less. This may be the reason that the rate of scale deposition comparatively falls off to some extent at higher rotational speeds.

In certain cases, the turbulence at high rotations (flow velocity) may act as a means of scale removal due to high shear forces, and as a result may wash away the freshly depositing layers of scale on the previously deposited scale (i.e., reverse of deposition process under favorable conditions due to high velocity). We observed breaking away of some tiny pieces of scale in the glass cell at high rotational speeds ($\geq$1,500 RPM), which may be due to scale removal process. Another reason could be that since the $CaSO_4$ crystals growth is of needle-type or acicular form (see morphology section), therefore, is susceptible to break away or dislodge at high velocity.

The above growth and dissolution mechanism from the incompatible waters or supersaturated solutions can briefly be summarized as:

- precipitation due to supersaturation,
- diffusion/transport of scaling species to the surface,
- adsorption of scalant on the surface to form ''adions'',

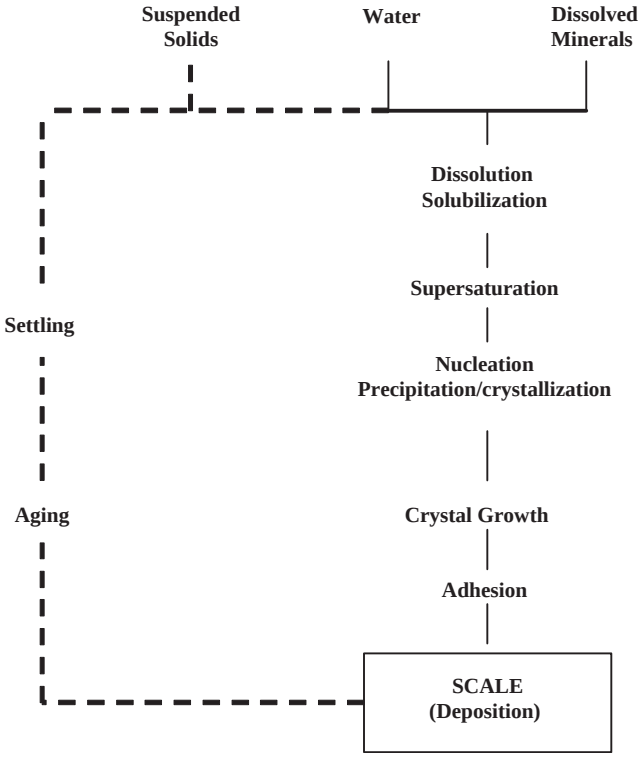

Fig. 4. Schematic representation of the scale deposition mechanism from process water/fluid system [2].

– incorporation of adions into the surface lattice of metal/ previous scale layer, and
– dissolution/removal process if favorable conditions exist (e.g., high velocity).

Fig. 5 presents a comparison, under identical experimental conditions, between the deposition rate of $CaSO_4$ scale on copper and stainless steel-316 [20]. The copper substrate shows comparatively more scale deposition than stainless steel-316, which is attributed to material characteristics such as surface activation energy and/or surface wetness. Therefore, the conditions for the deposition of scale on copper were more favorable compared to stainless steel which yielded more scale on copper.

We used pure salts without any external seeding or contamination in the present study. The seeding enhances the crystallization process [4–6]. The external impurities, such as particulates, suspended solids, mixed salts, corrosion products, biological matters, surface geometry and flow velocity, etc., play a significant role on the deposition behavior of scale on the surface and affect the overall growth rate of scale. If these conditions exist, the scaling/fouling rate may result in linear (increasing or falling) or asymptotic relationships

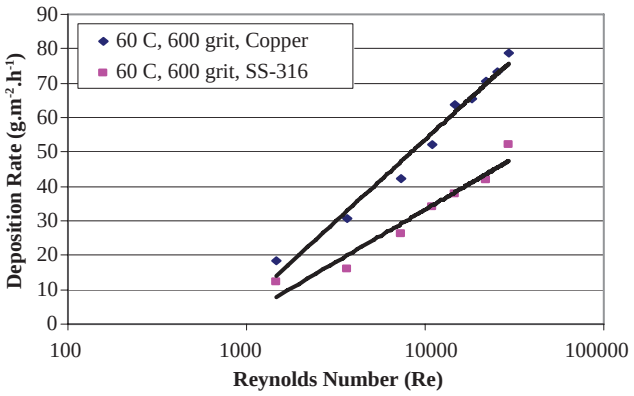

Fig. 5. Comparison of average deposition rate of calcium sulfate scale on copper and SS-316 [20].

[29,30]. In heat exchange equipment the asymptotic behavior of scaling/fouling is observed when the rate of deposition of scale is equal to the rate of removal of scale under appropriate fluid flow conditions.

3.2. Diffusional mass transport

Figs. 3 and 5 show that the $CaSO_4$ scaling rate increases with Reynolds number further suggesting that the deposition process is mass transport dependent. According to Levich analysis [31], under diffusional mass transport control conditions, the mass transfer coefficient should increase with $\sqrt{Re}$. Hence, if so, the plot of {log (deposition)} verses {log (Re)} should show a straight line with a theoretical slope of 0.5 [31].

To demonstrate this feature, Fig. 6 presents the results of log (deposition rate) vs. log (Re) for the data generated in the study for 60 and 70°C,. A straight line behavior can be seen from the figure with slopes of 0.486 for 120 grit surface polish and 0.469 for 600 surface polish at 60°C, and 0.466 for 600 grit polish samples at 70°C. The slopes of these best fitted lines are close to the theoretical value of 0.5, therefore, the results of the study corroborate the diffusion controlled mass transport aspect of the scale deposition process.

3.3. X-ray diffraction analysis

Phase identification of calcium sulfate scale was carried out using X-ray diffraction technique. The XRD spectra shown in Fig. 7 were generated and indexed for all possible forms of gypsum, included in the International Committee on Diffraction Database (ICDD) standards, i.e., for dihydrate ($CaSO_4{\cdot}2H_2O$), hemihydrate ($CaSO_4{\cdot}1/2H_2O$), $CaSO_4{\cdot}0.62H_2O$, $CaSO_4{\cdot}0.67H_2O$, $CaSO_4{\cdot}0.15H_2O$ and anhydrite ($CaSO_4$).

All peaks positions and relative intensity ratios in the XRD pattern obtained in the study matched with that of hemihydrate-$CaSO_4{\cdot}1/2H_2O$ (ICDD-PDF Card

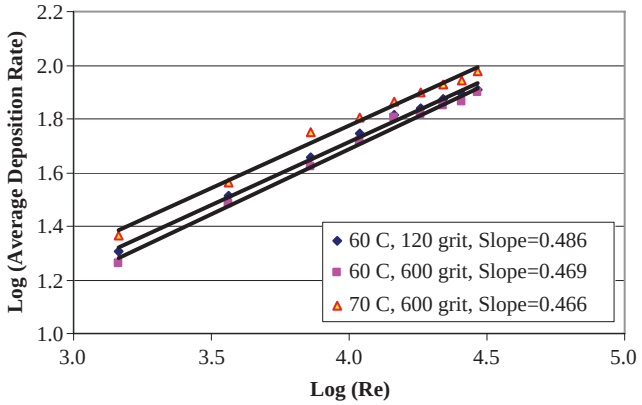

Fig. 6. Log–Log plot of average deposition rate vs. Reynolds number for calcium sulfate scale on copper.

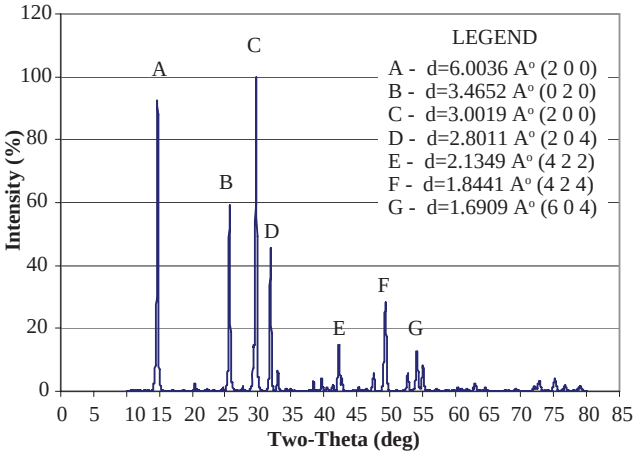

Fig. 7. XRD spectra of scale identified as calcium sulfate hemihydrate gypsum (ICDD Card 00-041-0224), in the study.

00-041-0224) standard. Therefore, by XRD analysis, the scale obtained was being identified as calcium sulfate hemihydrate ($CaSO_4 \cdot 1/2H_2O$) gypsum.

3.4. Morphology

The scanning electron microscopy examination of the gypsum scale crystals exhibited mainly prismatic needles and/or rods-like growth structures. However, at certain locations some flat crystals were also seen which had been formed due to the coagulation of prismatic rods. SEM examination in general showed that the $CaSO_4$ crystals initially started at the nucleation sites on the substrate surface or on the existing crystals and then branched out randomly in all directions. The energy dispersive X-rays diffraction spectroscopy (EDS) profile obtained on scaled copper specimen is shown in Fig. 8. The scale forming solution was prepared from pure chemicals, therefore, the large peaks for calcium (Ca), sulfur (S) and a small peak for oxygen (O) in the EDS spectra confirmed the nature of crystals as calcium sulfate ($CaSO_4$).

Fig. 9 presents some typical SEM results of the morphology of calcium sulfate crystals deposited on copper substrate after 1 and 2 h of exposure to the scale-forming solution. The scale crystals initially grow at the nucleation sites in the shape of tiny prisms which further develop into needles or prismatic rods and then join together to form flat crystals. The photomicrographs in Fig. 9(c) to (f) show a dense population of uniformly distributed CaSO4 crystals on the entire surface of the copper substrate. Similar results were obtained in earlier studies for the $SrSO_4$ [7], $BaSO_4$ [19] and $CaSO_4$ [20] scale deposition on Stainless Steel-316. The micrographs, however, further indicate the random growth of subsequent crystals emanating from either the nucleation sites (Fig. 9(b)) or the already deposited primary crystals (Fig. 9(c) to (f)). In addition, the secondary as well as perpendicular growth of $CaSO_4$ crystals is also evident in these micrographs (Fig. 9(b) & (f)). Fig. 9(b) shows the flower type random nucleation growth, as well. The crystals thus, seem to have been growing at preferential nucleation sites available on the substrate and/or previously deposited scale layer.

It is conjectured that once a basal layer of scale is formed the subsequent scale growth on it is much faster because of the readily available abundant nucleation sites as compared to a polished surface during the scale deposition process on metal surface. Moreover, the scaled surface becomes sufficiently rough with large surface area, which subsequently promotes deposition as compared to a bare or polished surface. The existing layers of scale provide more nucleation sites for further scale growth and adhesion on the substrate surface. These morphological results agree with

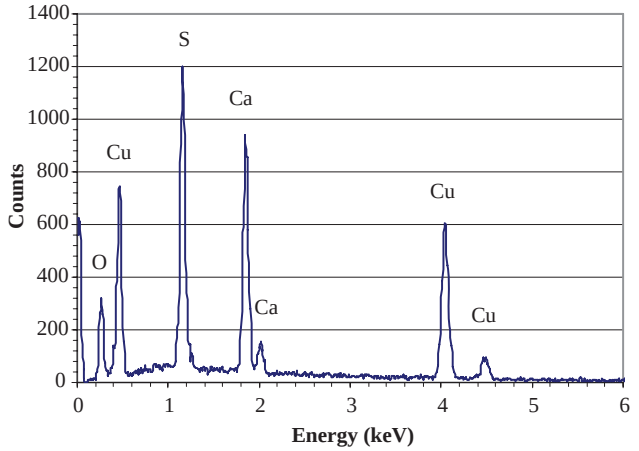

Fig. 8. EDS profile of calcium sulfate scale crystals deposited on copper.

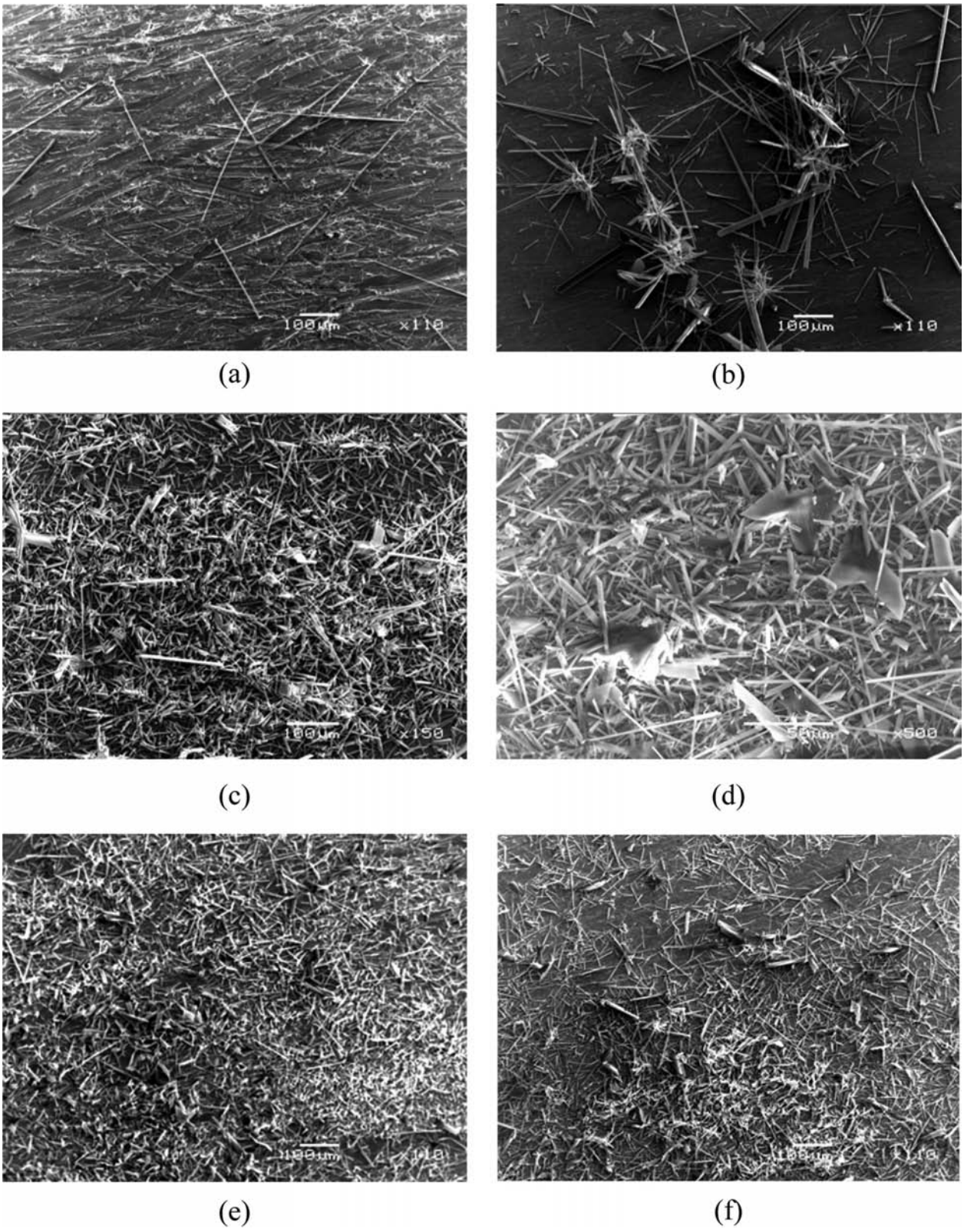

Fig. 9. SEM micrographs showing the morphology and distribution of $CaSO_4$ crystals on copper substrate [120 grit-polish-(a) & (d); and 600 grit-polish-(b), (c) (e), and (f)]. (a) Morphology (few prismatic needles) – after 1 h, (b) Morphology (needles & rods) random and perpendicular growth at nucleating sites – after 1 h, (c) General morphology (needles & flat plates) – after 1 h, (d) to (f) General morphology (prismatic needles, rods and flat plates) – after 2 h.

the earlier studies [7,9,20]. The reason seems to be a random growth of the subsequent crystallites on the previously deposited scale crystals, i.e., a sort of epitaxial growth, as revealed from the SEM micrographs (Fig. 9), which promotes scale deposition process.

5. Conclusions

The turbulent mixing due to the agitation of the solution promoted scale formation by allowing more active scale-forming species to adsorb on the metal surface that ultimately deposited and adhered on copper substrate. Hydrodynamics of the solution plays a vital role in scale deposition process, therefore, it must be a part and parcel of any water treatment, scale squeeze or scale prognostic model.

The replenishment of fresh solution to the test cell provided constant ionic chemistry for the scale deposition throughout the experimental runs.

The effect of surface roughness on the deposition of calcium sulfate scale on copper was conspicuous. The 120 grit polished samples showed comparatively more scale than 600 grit polished copper specimens.

The deposition of calcium sulfate scale on copper was significantly higher as compared to stainless steel-316 under identical test conditions.

The effect of temperature increase has a significant impact on scale deposition because of the inverse solubility effect of supersaturated scaling solution. At 70°C more deposition of calcium sulfate scale on copper was observed than at 60°C at the same test conditions.

The scale deposition rate versus Reynolds number showed an increasing trend for the data developed in the present work; however, in practical industrial situations, the deposition may likely show a different behavior, e.g., falling or asymptotic rate. The data presented further supports the diffusion controlled mass transfer process.

The SEM examination revealed prismatic needles, rods and flat crystal structures. The growth of $CaSO_4$ crystals initially started at the nucleation sites present on the specimen surface and then branched out randomly in all directions. Flower shaped crystals emanating from nucleating sites were evident at certain locations. In addition, growth of secondary crystals of scale on the primary crystals was also observed from SEM micrographs. The XRD analysis identified the scale as hemihydrate ($CaSO_4 \cdot 1/2H_2O$) gypsum.

Acknowledgement

The support of the Ministry of Higher Education and the Research Institute of King Fahd University of Petroleum and Minerals for this work is highly acknowledged.

Symbols

aq	Aqueous
s	Solid
Re	Reynolds number (dimensionless)

References

[1] D.E. Potts, R.C. Ahlert and S.S. Wang, Desalination, 36 (1981) 235–264.
[2] J.C. Cowan and D.J. Weintritt, (Eds.), Water Formed Scale Deposits, Gulf Publishing Co., Houston, Texas, (1976).
[3] M. Al-Ahmed and F.A. Aleem, Desalination, 93 (1993) 287–310.
[4] P.A. Read and J.K. Ringen, SPE 10593, Presented at 6th International Symposium on Oilfield and Geothermal Chemistry, Dallas-Taxes, January 25-27, 1982, pp. 7–17.
[5] G.H. Nancollas, Croatica Chem. Acta, 43 (1973) 225–231.
[6] Sung-Tsuen Liu and G.H. Nancollas, J. Crystal Growth, 6 (1970) 281–289.
[7] M.I. Khokhar, S.K. Somuah, M.O. Amabeoku, I.M. Allam and A. Quddus, Proc. 4th Middle East Corrosion Conference, Bahrain, January 11–13,1988, Part 1, pp. 244–258.
[8] S.M. Zubair, A.K. Sheikh, M.O. Budair, M.U. Haq, A. Quddus and O.A. Ashiru, J. Heat Transfer (Trans. ASME), 119 (1997) 581–588.
[9] M.O. Budair, M.S. Sultan, S.M. Zubair, A.K. Skiekh and A. Quddus, J. Heat & Mass Transfer, 34 (1998) 163–170.
[10] D. Hasson, M. Avriel, W. Resnick, T. Rosenman and S Windreich, I and EC Fundamentals, 7, No. 1 (1968) 59–65.
[11] D. Hasson and J. Zahavi, I and EC Fundamentals, 9, No. 1 (1970) 1–10.
[12] G. Liu, D.A. Tree and M.S. High, Corrosion, 50 (1994) 584–593.
[13] K.D. Efrid, E.J. Wrright, J.A. Boros and T.G. Hailey, Corrosion, 49 (1993) 992–1003.
[14] D.C. Silverman, Corrosion, 40 (1984) 220–226.
[15] D.C. Silverman, Corrosion, 44 (1988) 42–49.
[16] D.R. Gabe, J. Appl. Electrochem., 4 (1974) 91–108.
[17] O.A. Ashiru and J.P.G. Farr, J. Electrochem. Soc., 139, No. 10 (1992) 2806–2810.
[18] C.T.J. Low, C.P. de Leon and F.C. Walsh, Aust. J. Chem., 58 (2005) 246–262.
[19] A. Quddus and I. M. Allam, Desalination, 127 (2000) 219–224.
[20] A. Quddus, Desalination, 142 (2002) 57–63.
[21] A. Quddus and L.M. Al-Hadhrami, Desalination, 246 (2009) 526–533.
[22] A. Neville, A.P. Morizot and T. Hodgkiess, Mater. Perform., 37, No. 5 (1998) 50–57.
[23] A. Neville, A.P. Morizot and T. Hodgkiess, J. Appl. Electrochem., 37, No. 4 (1999) 455–62.
[24] A. Neville and A.P. Morizot, J. Crystal Growth, 345 (2002) 490–502.
[25] A. Morizot, A. Neville and T. Hodgkiess, J. Crystal Growth, 198/199 (1999) 738–743.
[26] T. Chen, A. Neville and M. Yuan, J. Petroleum Sci. Eng., 46 (2005) 185–194.
[27] R.P. Singh and N.M. Abbas, Proc. 5th Middle East Corrosion Conference, Bahrain, October 28-30, 1991, Vol. 4, pp. 561–569.
[28] T.R. Bott,. Fouling of Heat Exchangers, Elsevier, Netherlands, 1995.
[29] G.F. Hewitt (Ed.), Hemisphere Handbook of Heat Exchanger Design, Section 3.17, Hemisphere Publishing Corporation, New York USA, (1990).
[30] J.G. Knudsen, Proc., the 20th ASME/AIChE Heat Transfer Conference, Milwaukee-Wisconsin, August 2-5, 1981, HTD-Vol. 17, pp. 29–38.
[31] V.G. Levich, Physicochemical Hydrodynamics, Prentice-Hall, Englewood Cliff, N.J., 1962.